

2 Lab 1: An Exploration of Atomic Force Microscopy (AFM)

3 SHRIHAN AGARWAL¹

4 ¹ University of California, Berkeley, Department of Astronomy, Berkeley, CA 94720

5 Abstract

6 We delve into an exploration of atomic force microscopy (AFM), its versatility and uses. Further,
7 we explore physical properties such as the Boltzmann constant and the atomic force regime. We
8 investigate the working principle of CDs and DVDs and find agreement in their standardized track
9 width and spacing. We study polymer glue and use AFM to distinguish between various polymer
10 components. We investigate forces as a function of distance in the atomic regime, and find a region
11 of attractive force before a stronger repulsive force as we approach the material surface. Lastly, we
12 estimate the Boltzmann constant using deflections of the cantilever, and found that the Boltzmann
13 constant was $k_B = 1.497^{+0.218}_{-0.182} \times 10^{23} \text{ J/K}$, in agreement with the expected value withing 1-sigma.
14 Atomic Force Microscopy is shown to be a versatile, capable instrument with a plethora of current and
future uses.

15 1. INTRODUCTION

16 Atomic Force Microscopy is a method of imaging the texture and material characteristics of objects from nanometer
17 to micron scale by measuring the atomic forces on a microscopic cantilever probe. A versatile instrument, the
18 AFM can measure the vertical dimension of the sample, works on electrically non-conductive materials, and even
19 through a liquid medium, e.g. water. With this diverse set of capabilities, it is used in scientific and engineering
20 fields across the board, such as biophysics. In many fields of science today, the AFM has taken the lead over pure
21 imaging devices such as electron microscopes (SEM and TEM). The minimal sample preparation required for an AFM,
22 and its large versatility for a variety of different samples conductive and non-conductive, make it particularly appealing.

23 Some of the most advanced AFMs in the field of research today have reached picometer levels of precision, and have
24 more recently been used to scan a wider variety of properties and actively manipulate surfaces and small particles.
25 Data acquisition speeds can now be in the millisecond range, enabling the visualization of the dynamic behavior of
26 biological molecules and cells. 3D mapping of surface forces, and detection of particular chemical bonds has also been
27 achieved (Min 2022).

28 In this lab, we seek to accomplish multiple objectives to both explore atomic force microscopy and its capabilities,
29 while also exploring different surfaces, and their material. First, we explore the noise floor of the AFM using a blank
30 Silicon wafer sample. Second, we use the 3D surface scan capabilities to investigate the function of CDs and DVDs.
31 Third, we seek to distinguish different materials on a polymer glue sample using phase detection. Fourth, we study the
32 trend of attractive and repulsive intermolecular forces at close distances with AFM-generated Force-Distance Graphs.
33 Lastly, we determine the Boltzmann constant by precisely measuring the fluctuations of the cantilever of the Atomic
34 Force Microscope.

35 We briefly describe Background Research Theory on AFMs in Section 2. We discuss the experimental design for
36 the various analyses in Section 3. The raw data collected is described in Section 4. Our analysis of the force surfaces,
37 alongside the estimate of the force-distance graphs and Boltzmann constant, are in Section 5. Lastly, the conclusions

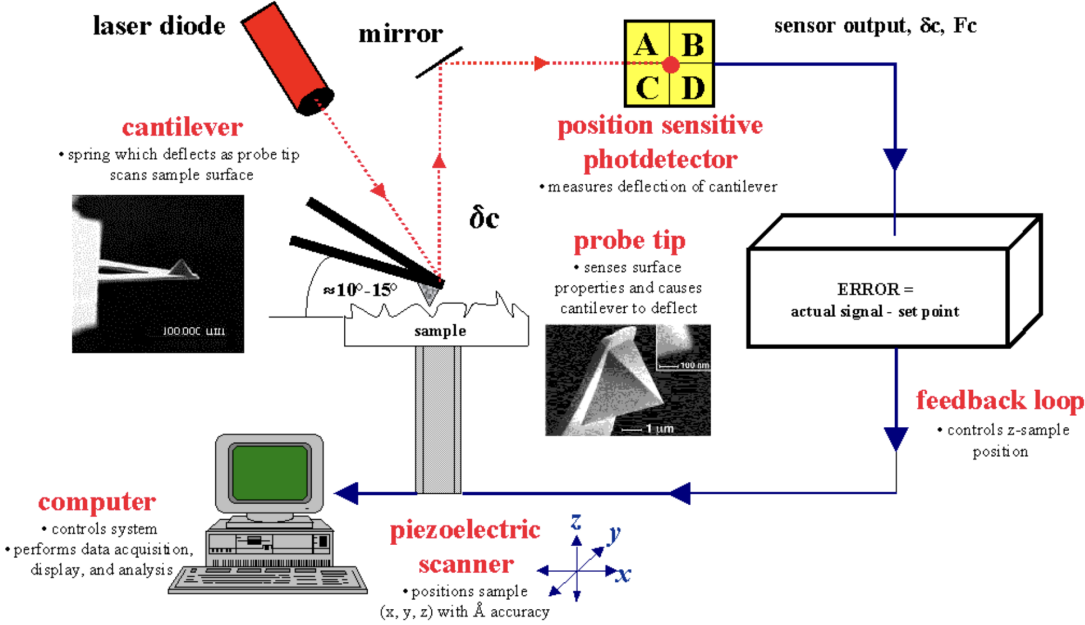


Figure 1: A model diagram describing the working principle of an atomic force microscope. The cantilever probe tip (in black) is placed close to the sample. The laser diode emits a focused beam whose deflection is amplified by the mirror and measured by the photodetector. The sensor outputs a voltage corresponding to the cantilever deflection, and either adjusts the piezoelectric scanner on which the sample is placed to bring the probe tip closer, or can send the data to the computer.

41 are presented in Section 6.

42

43

2. BACKGROUND RESEARCH AND THEORY

2.1. Instrument Mechanism

44 The principle on which an Atomic Force Microscope functions is that atomic forces from a sample can affect a probe placed near it. This probe is composed of a sharp tip attached to a cantilever, and is of nearly micrometer size in order to measure samples at that precision. The cantilever deflects as a function of the forces on it, and this deflection is captured by use of a laser and position-sensitive detector that reflect off of the back of the tip. As such, when the tip deflects, the laser light also deflects on the detector. A diagram of this is presented in Figure 1, referenced from the corresponding slide in the lab manual. The laser light from the diode deflects proportionally in accordance with the cantilever deflection, but is amplified by the mirror and measured by the position sensitive photodetector. A highly precise detector, it compares the detector brightness in the top and bottom detector plates and generates a corresponding T-B (top - bottom) voltage, which can be extracted directly or observed on a computer. Later in this lab, we connect this external voltage to a low-noise amplifier and a spectrum analyzer to understand the typical cantilever deflection when not being driven.

45
46
47
48
49
50
51
52
53
54
55
56
57
58
59
60
61
62
63
64
65 There are two modes of operation of the atomic force microscope: Vibrating Mode (Non-Contact) and Non-Vibrating Mode (Contact). In Vibrating mode, the AFM cantilever remains suspended in the attractive regime of atomic force, slightly above the surface, and is driven at a particular frequency near the natural resonance frequency of the cantilever. If the atomic force increases or decreases, usually due to a change in the vertical height of the surface, the amplitude of the oscillation correspondingly increases or decreases, in accordance with the principle of a driving force on an oscillating body. This change in amplitude can be measured by the detector and compensated for by moving the Z-piezo stage on which the sample is placed up or down. The height of the Z-piezo stage during this raster scan can populate an image with a measurement of the atomic force corresponding to the Z-piezo height at numerous x and y positions on the sample surface. In contact mode, the cantilever is Non-Vibrating, and is placed in the repulsive

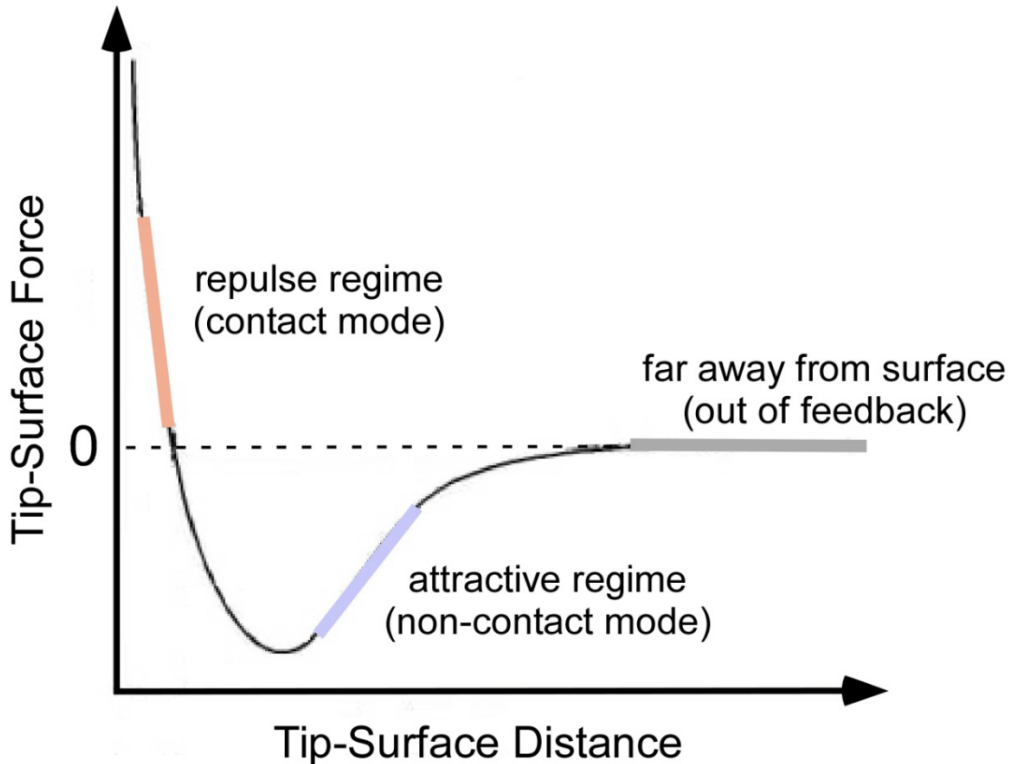


Figure 2: A model diagram describing the attractive and repulsive regime of the atomic force microscope. At a far distance, there is no contact or atomic force, and no deflection is observed. As the tip gets closer, there is a short attractive Van der Walls regime in which the tip is pulled to the surface, beyond which repulsive atomic forces begin to take over (Lecture Slides, AFM).

regime, closer to the sample surface. The degree of deflection of the cantilever is responsible for the measurement of the atomic forces, as a peak would cause a large deflection and hence force measurement. A diagram approximately describing the structure of the attractive and repulsive regime is shown in Figure 2.

70 2.2. AFM Components

71 The atomic force microscope uses multiple components to satisfy the working principle of the instrument. We
72 describe the various components of the atomic force microscope below.

- 73 • AFM Probe - The probe is a thin strip composed of a cantilever and a tip, which is attached to the end of the
74 AFM machine and vibrates to create the necessary measurements. It is generally made of silicon, and frequently
75 coated with diamond, gold, or is sharpened. The tip itself is attached to a larger carrier chip, to which the clasp
76 of the probe holder is attached.
- 77 • Probe Holder - The probe is attached to the probe holder for input into the microscope setup. The probe can
78 be added to the probe holder through a careful procedure as described in the following Section 3.
- 79 • AFM Sample Holder - The stage on which the sample is placed. The sample holder can translate in 3 dimensions
80 allowing precise movement of the sample to the probe in the location of interest. The sample holder is connected
81 to a stage that performs these precise translations. We move this stage with manual knobs or using computer
82 inputs. The scanning stage uses the piezoelectric effect, which creates a stress or strain in response to an electrical
83 signal, stretching or compressing the piezoelectric stage highly precisely.

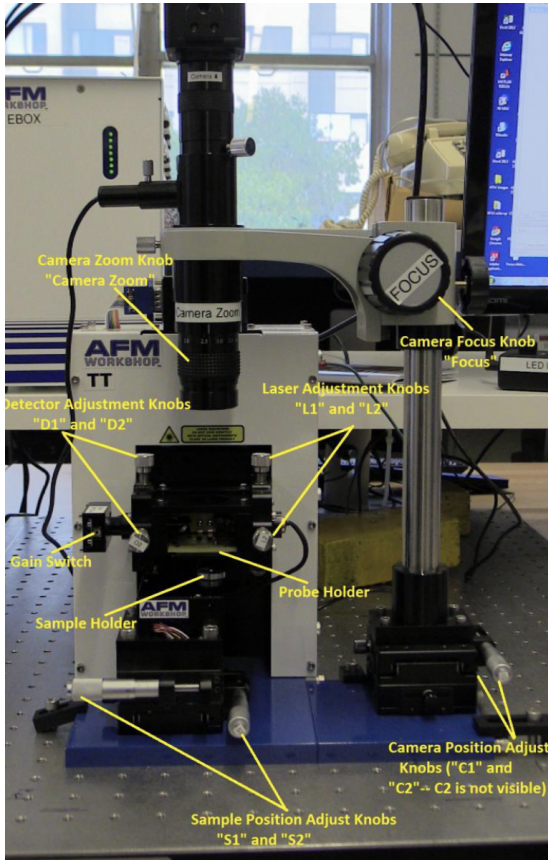


Figure 3: The various components of the atomic force microscope are shown in the image above (drawn from the Lab Manual).

- 84 • Light Probe and Dectector - The laser diode and detector, or the corresponding mirrors, can be moved up and
85 down with the help of knobs or a coarse stepper motors to calibrate the instrument.
- 86 • Video Optical Microscope - The video optical microscope probes roughly the same degree of magnification as
87 the AFM, and is hence used in combination with the AFM to help locate features on the surface to be scanned,
88 avoid artifacts or broken portions of the sample, and ensure the laser diode calibrations are done correctly.
- 89 • Electronics and EBOX - The EBOX placed behind the AFM is responsible for controlling and performing the
90 data acquisition, responsible for interfacing the device with the computer. It also directly outputs the T-B
91 voltage detected from the AFM, which is used later in Section 3.
- 92 • Software - The calibration and software required to drive the instrument are provided as a LabVIEW program.
93 It is the interface for the instrument calibration, pre-scan setup, and input of scan settings.

94 2.3. CD and DVD

95 The CD stores data on its surface. The information is stored on a single long spiral track going from the inside to
96 the outside. This spiral track is composed of small bumps and pits which correspond to 0s and 1s, and can be read
97 out as data by a CD reader. The pits of the CD are typically 125 nm deep and 500 nm wide. Their length can vary
98 anywhere from 850 nm to 3500 nm (3.5 micrometers). The spacing between the tracks is 1.6 μm . Similarly to an
99 AFM itself, the presence of the pits and bumps can be determined by a small reflective laser shined on the CD. If a
100 pit appears, the light's position on the detector changes. This light is an 780 nm for a CD.

101 The DVD is a more compressed version of the CD format, and can store more information. However, it also requires
102 a more efficient reader. The bumps are shorter, now only 400 nm long. And the spiral track's pitch is now 0.74 μm , a

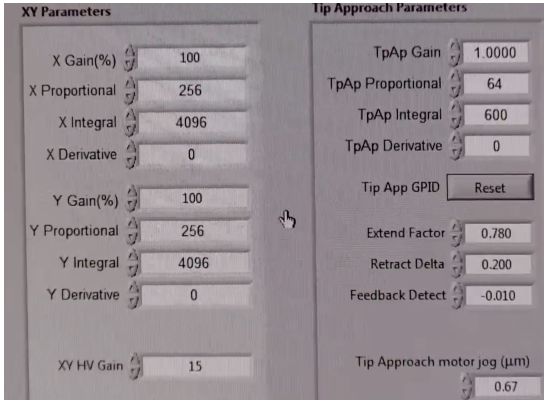


Figure 4: The settings for the AFM tip approach and XY chosen for our experiment.

reduction from the $1.6 \mu\text{m}$ of CDs. In order to read this, the DVD has an even higher frequency wavelength of light used - 650nm, which is in fact visible as red light. In this lab, we use a Blue-ray DVD. This DVD uses an even higher frequency: 405nm, operating in the blue-violet region, and is even further compressed. We will attempt to verify these distances in our measurements of the CD and DVD surface.

2.4. Equipartition Theorem and the Boltzmann Constant

One of the primary goals of this experiment is to estimate the Boltzmann constant. The oscillations of the cantilever can be precisely measured. Knowing the equipartition theorem from statistical mechanics,

$$\frac{1}{2}k_B T = \frac{1}{2}k \langle z^2 \rangle$$

, where k_B is the Boltzmann constant, k is the spring constant of the cantilever, and T is the temperature in Kelvin, and $\langle z^2 \rangle$ is the root mean squared deflection of the cantilever. This equation arises from the fact that the cantilever (or any spring) naturally oscillates at a particular natural frequency (the resonance frequency), with an oscillating energy that can be made equal to the equipartition theorem for one degree of freedom. At higher temperatures, this oscillation would increase. Given the temperature, spring constant, and root mean squared deflection, we can estimate the Boltzmann constant using the AFM,

$$k_B = \frac{k \langle z^2 \rangle}{T}.$$

Here, $\langle z^2 \rangle$ can be measured as the integral of the power spectrum at the resonance frequency,

$$\langle z^2 \rangle \propto P_{res} = \int_{f_r-w_r}^{f_r+w_r} P(f) df$$

, and z^2 can be correlated with V^2 from the appropriate force-distance graph obtained from analysis to obtain the constant of proportionality. See Section 5.

3. EXPERIMENTAL DESIGN

3.1. General Experimental Setup

In general, the typical procedure of atomic force microscope setup proceeds as follows for the majority of experiments in this report. The components of the AFM and the relevant knobs are presented in the Figure 4.

- We take care to safety first, and note the presence of a laser in the AFM setup. We ensure that we take care to turn off the laser when taking the probe holder in and out from the setup, or while placing the sample in the holder. If not, we may accidentally cause reflections of laser light into our eyes.
- We power on the EBOX device connected to the AFM. If necessary, we restart it in case the program hangs or troubleshooting is required.

- We open the Optical Microscope video viewer on the computer, and adjust the LED illuminator lighting such that the tip of the probe is visible. This may need to be readjusted once the sample is placed, depending on the transparency of the material.
- We open the LabVIEW program to control and drive the AFM. We hold the Manual Z Motor Control up and down buttons to ensure the device is working correctly, and can hear the motor move the Z-piezo stage accordingly.
- If necessary, we perform a probe exchange by taking the probe holder and placing it on the probe exchange tool. Carefully applying force to the sides of the probe holder, the probe can be removed from its clasp. The new probe can be placed with precise and careful use of tweezers specifically capable for this purpose, and the probe holder can be reinserted into the microscope. We adjust the focus of the optical microscope to ensure the tip is appropriately positioned and not clearly damaged.
- The laser diode is turned on using the AFM software, and the laser light is repositioned onto the tip of the cantilever (L1 and L2 knobs). The detector is then positioned such that the default T-B voltage is 0.4 V and the default L-R voltage is 0 V, using the D1 and D2 knobs. See Figure 4.
- The sample is then carefully placed onto the sample holder using a pair of tweezers. The optical microscope is refocused onto the sample surface.
- If in Vibrating mode, the tip is tuned by searching the range of allowed frequencies for the oscillating tip and finding the resonant peak. We set the oscillating frequency to that of the peak and ensure the phase is anti-symmetric.
- The settings of the AFM Calibration tab are checked in order to ensure they match the expected values, as seen in Figure ??.
- A range check is performed with the AFM after ensuring it is well above the sample.
- The tip is brought to the sample using the knob until the tip comes into view in the optical microscope. We then use the Manual Z Motor Control in the LabVIEW program until the tip comes well into focus. To ensure that the tip is not broken, we begin the Automated Tip Approach at this stage. We change the Z HV Gain to 15 in order to speed up the tip-approach process.
- Once the tip approach is complete, an "in-feedback" indicator is turned on, and the scan may begin. If the Z-measured voltage is positive, the AFM is very slightly dropped until the voltage falls into the negative range. We specify the details of each scan in the following sections.

3.2. Calibration

Beyond the typical procedure, the calibration was performed on a clear region of Sample 7 Feature B. This sample consisted of square pits with $10 \mu\text{m}$ width and 100 nm depth, a useful calibration sample to check the functioning of the AFM.

We performed 4 sets of scans. Aligning the sample with the AFM probe X and Y carefully using a tweezer, we performed 2 scans of $25 \mu\text{m}$ width at a scan rotation of 0 degrees, and 2 scans of $25 \mu\text{m}$ width at a scan rotation of 90 degrees. The process took about 4 minutes per scan, with 256 scan lines at 1 Hz. Due to the presence of dust and other particles, the best profile of square pits was carefully chosen.

Examining the profile of the square pits in Gwyddion, we performed a leveling procedure on the Z-DRIVE measurement of the AFM, which is a measure of the height of the Z-piezo during non-contact mode. Post leveling, we drew a line profile through the best set of squares and used this to determine the X and Y calibration. Since the AFM did not output exact values such as $10 \mu\text{m}$ width, and instead outputted approximately $9.7 \mu\text{m}$ in X and $11.3 \mu\text{m}$ in Y, we decided that calibration was required. The exact measurements are provided in Figure 5.

Piezo	System Cal	Measures1	Measures2	Measures3	Measures4	Actual
X	0.521404	9.7	9.86	9.82	9.68	10
Y	0.578399	10.93	11.99	12.1	11.71	10
Z	0.595729	91.4	91.8	86.9	92.2	100
						Set XY

New X: 0.5088561310803892
New Y: 0.6616993481703403
New Z: 0.6577190173889041

Figure 5: The calibration settings for the AFM before and after the update.

We replaced the calibration parameters in the AFM settings with the new calibration values in Figure 5 before beginning our experiment on each iteration. This improved the quality of the measurement and reduced distortions in the imaging for all future experiments.

3.3. Noise Floor

Another goal of our exploration is to accurately determine the noise floor of the AFM. By carefully considering the noise floor of all internal and external sources of noise, we may more accurately be able to determine signal from typical noise, while also identifying ways to reduce it. We utilize Sample 8, the Blank Silicon Wafer for this experiment.

The procedure is as follows:

- We change the XY HV Gain to 0 and Z HV Gain to 15 in the System Tab. Since the XY HV Gain is set to 0, the tip does not move on starting a raster scan.
 - We search for a clean region of the sample and perform a vibrating tip approach.
 - We perform 2 scans. The first, with minimal sources of noise - keeping the box housing the AFM closed, no tapping on the desk, and reducing any vibrations, including talking. For the second scan, we deliberately induce these vibrations, while keeping the box closed, taking care not to damage the instrument itself.
 - The following parameters are selected for the scan, although we do not wait for the scan to complete all 512 lines, and stop near 50:
 - Scan Size = 0.5 microns
 - Scan Rate = 1 Hz
 - Scan Lines = 512
 - X, Y Center = (2, 2)
 - Left, Right Image = Z-DRIVE, Z-ERR
 - We repeat the previous steps at a Z HV Gain of 5.

¹⁹⁹ The results from this experiment are analyzed in Gwyddeon in Section 5.

3.4. CD/DVD Experiment

The CD/DVD experiment involves the manual creation of a sample by extracting it from the CD manually, else the material oxidizes rapidly over the course of a week. We complete the sample preparation and experiment in a single day in order to avoid any artifacts from oxidation.

The CD sample is prepared with the following process:

- A double sided tape is attached to the magnetic sample plate on which the sample is to be placed. Any excess tape is cut off the sides.
 - A sharp X-acto knife is used to extract a small square from the central region of the CD with tweezers.

- 209 • It is placed on the tape shiny-side up, taking care to ensure the surface is as flat as possible, even if this
 210 necessitates damages to the edges of the sample.

211 The CD sample is scanned with a scan size of $15 \mu\text{m}$, with 256 scan lines and a scan rate of 0.5 Hz. The scanning
 212 process took 8 minutes.

213 For the DVD, the samples were already available, however, heavily damaged. It took significant effort combining the
 214 LED illuminator, optical microscope, and sample handling to ensure that the tip landed on a relatively clean region
 215 of the sample. The DVD was scanned with similar settings to the CD.

216 3.5. Polymer Glue

217 Although the polymer glue setup largely followed that of the general experiment, we opted for a Scan Size of $10 \mu\text{m}$
 218 and a Scan Rate of 0.5 Hz. Z-DRIVE and Z-PHASE were selected, the phase allowing the detection of different
 219 possible materials in the hot glue surface.

220 3.6. Force-Distance Curve Experiment

221 The Force-Distance curves are measured by considering the cantilever deflection as the cantilever approaches the
 222 surface in Contact mode. We seek to recreate Figure 2 experimentally. We use the Force-Distance Tab of the AFM
 223 LabVIEW program as follows,

- 224 • We find a clean region on the blank silicon wafer sample, and switch to Non-Vibrating Mode.
- 225 • We set the Reverse Trigger to T-B signal a 200 mV higher than the current set point. Going any higher than
 200 mV caused worse results, and any lower caused the program to not produce results for all z.
- 226 • We set the Vertical Axis to the T-B voltage output of the AFM detector. We take the data in the Slow setting.
- 227 • We take a small raster scan to populate the screen on the bottom-left of the Force-Distance tab. In it, we select
 228 a clean region of the sample to test.
- 229 • We take care not to type, impact the table or induce vibrations during this process.
- 230 • We take 8 curves and average their results in Section 5.

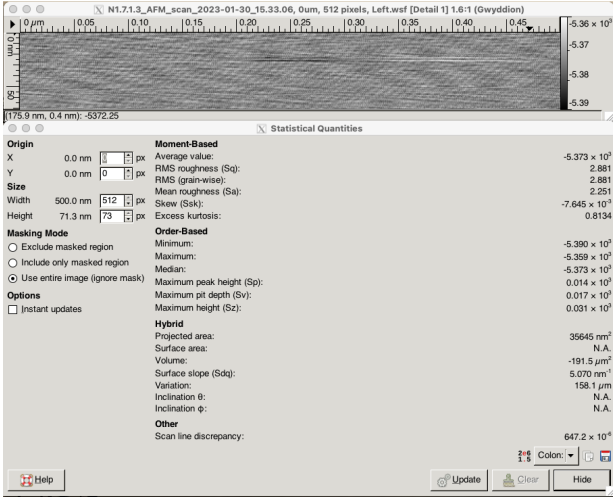
232 With an accurate Force-Distance curve, we can infer the relation between the T-B Voltage induced by the oscillations,
 233 and the true oscillations of the sample.

234 3.7. Boltzmann Constant

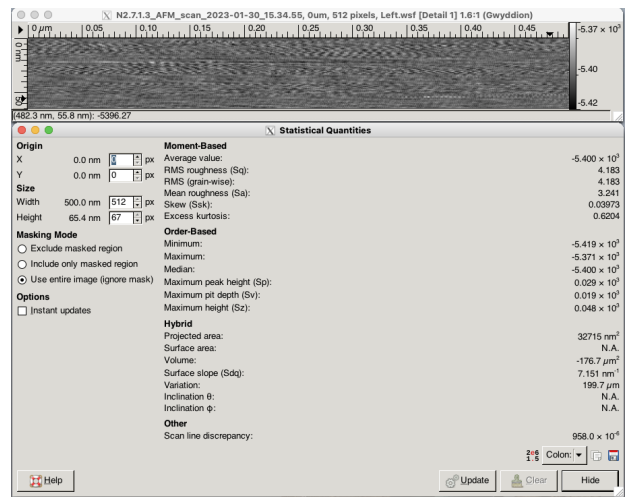
235 The Boltzmann Constant experiment required the use of additional components, namely a low-noise amplifier and
 236 a Spectrum Analyzer (SSA3021X Plus). We describe the following procedure in detail:

- 237 • We attach the T-B Voltage output of the EBOX to the low noise amplifier, set the low and high cutoff filters to
 300 Hz and 1MHz respectively and add a Gain of 100. This is necessitated in order to amplify the signal of the
 natural vibrations of the probe from typical noise in the experimental setup.
- 238 • The output of this amplifier is connected to the RF Input of the Spectrum Analyzer.
- 239 • Ensuring the cantilever is not being driven by the program, we switch the LabVIEW program to non-contact
 mode, and turn on the laser.
- 240 • In the Spectrum Analyzer, we zoom into the range near the peak of the natural resonance. We specifically search
 241 the region near the resonance frequency known from previous tuning of the probe tip.
- 242 • Once the peak is found, we select the Average setting in the bottom left of the Spectrum Analyzer, to Average
 over 1000 samples.
- 243 • Setting the Y-axis scale to Power, and the scale to Linear, we identify a clear peak at 180kHz. In this region,
 244 we zoom as much as possible to capture the best resolution possible near the resonance peak.
- 245 • The results from averaging are saved to a .csv file and analyzed with Python in Section 5.

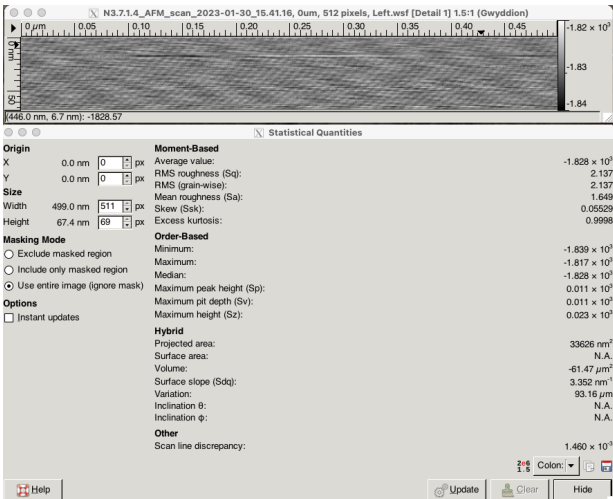
246 This approach allows us to obtain a power spectrum of the cantilever deflections, which can be converted to $\langle z^2 \rangle$.



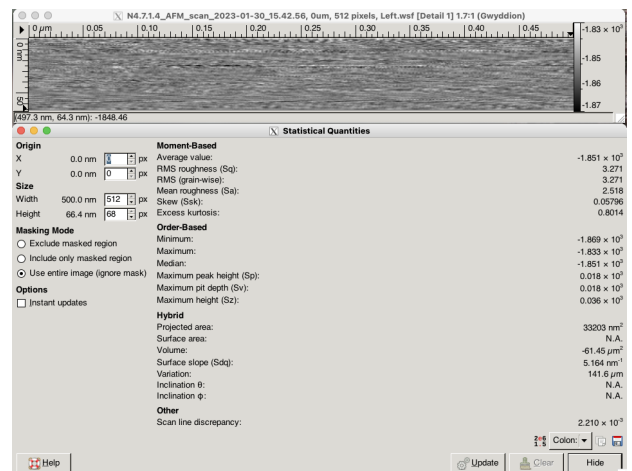
(a) Z HV Gain = 15, Clean, Mean Roughness: 2.251



(b) Z HV Gain = 15, Noisy, Mean Roughness: 3.241



(c) Z HV Gain = 5, Clean, Mean Roughness: 1.649



(d) Z HV Gain = 5, Noisy, Mean Roughness: 2.518

Figure 6: Noise Floor for different combinations of Z Gain and External Noise. Though these may not be visually comparable due to the differences in colorbar scaling, the mean roughness and other parameters describe the significant difference between the noise in both cases.

4. RAW DATA

4.1. Noise Floor

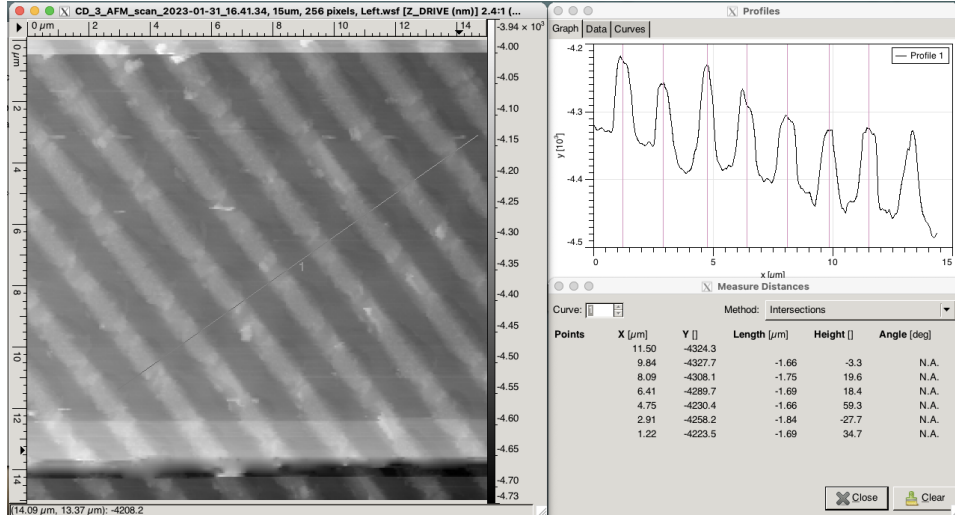
The noise floor of the experiment can be seen by the average value of the noise and the mean and standard deviation of the roughness. We can conclude that with a lower Z HV Gain, the noise is significantly reduced, and is the primary factor to reduce the noise floor. By reducing external noise, we can also see a drop in the typical noise.

4.2. CD/DVD Experiment

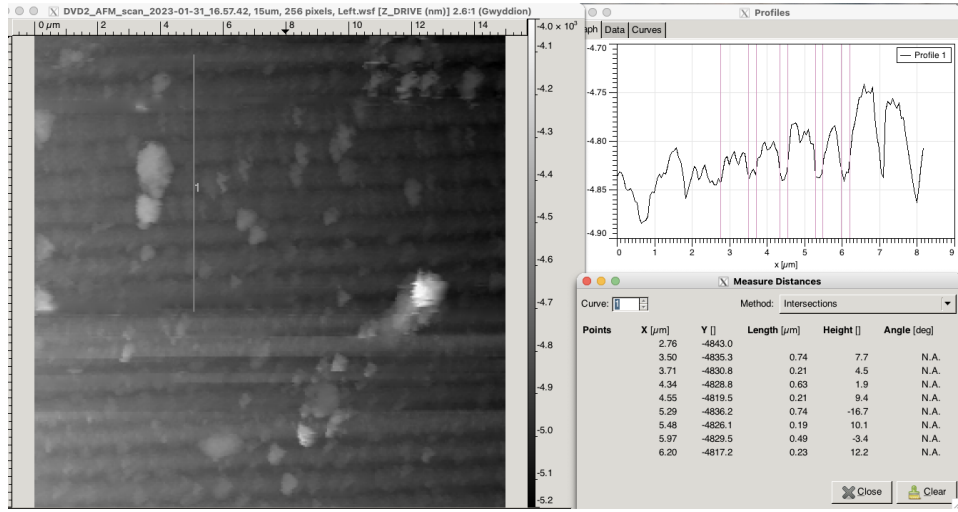
The CD and DVD can qualitatively be compared and we immediately notice the larger tracks and spacing for the CD, compared to the thinner and smaller pits and track spacing of the DVD, which carries significantly more information.

4.3. Polymer Glue

The Z-DRIVE and Z-PHASE are plotted side by side in the Figure 8. We notice that the features in the phase image do not necessarily correlate with the drive image, indicating that not all of the peaks are dust. Within the hot glue, we can see multiple different kinds of polymers that are distributed independently of the z-height of the surface -



(a) CD Surface and Line Profile



(b) DVD Surface and Line Profile

Figure 7: The CD and DVD surfaces are on the left, while the depth and width of the DVD pits can be seen on the right. We can qualitatively notice that the CD tracks are much less dense and concentrated, and are also larger compared to the DVD. Though we cannot detect the individual pits, the track width and spacing can be calculated in Section 5.

this is why the two are not necessarily correlated. The increase in phase corresponds to an increase in softness of the sample. We can make our 4 different polymers in the phase images: orange, bright yellow, black and brown.

4.4. Force-Distance Graphs

We aggregate the 8 force-distance curves in the Figure 9. They are matched up correspondingly by shifting them according to their mean in the no-force regime. Here, the x-axis is in nm, and the y-axis is in V. We can see a clear dip in the curve, marking the attractive phase of the regime.

4.5. Boltzmann Constant Estimation

We find the Power Spectrum .csv file saved from the Spectrum Analyzer to have the graph in Figure 10. The frequency decomposition has a sharp peak at the region of interest, and is 0 elsewhere. This can be integrated over without significant difficulty. The uncertainties in the Spectrum Analysis are hard to discern, but were capped at 0.01 W/Hz.

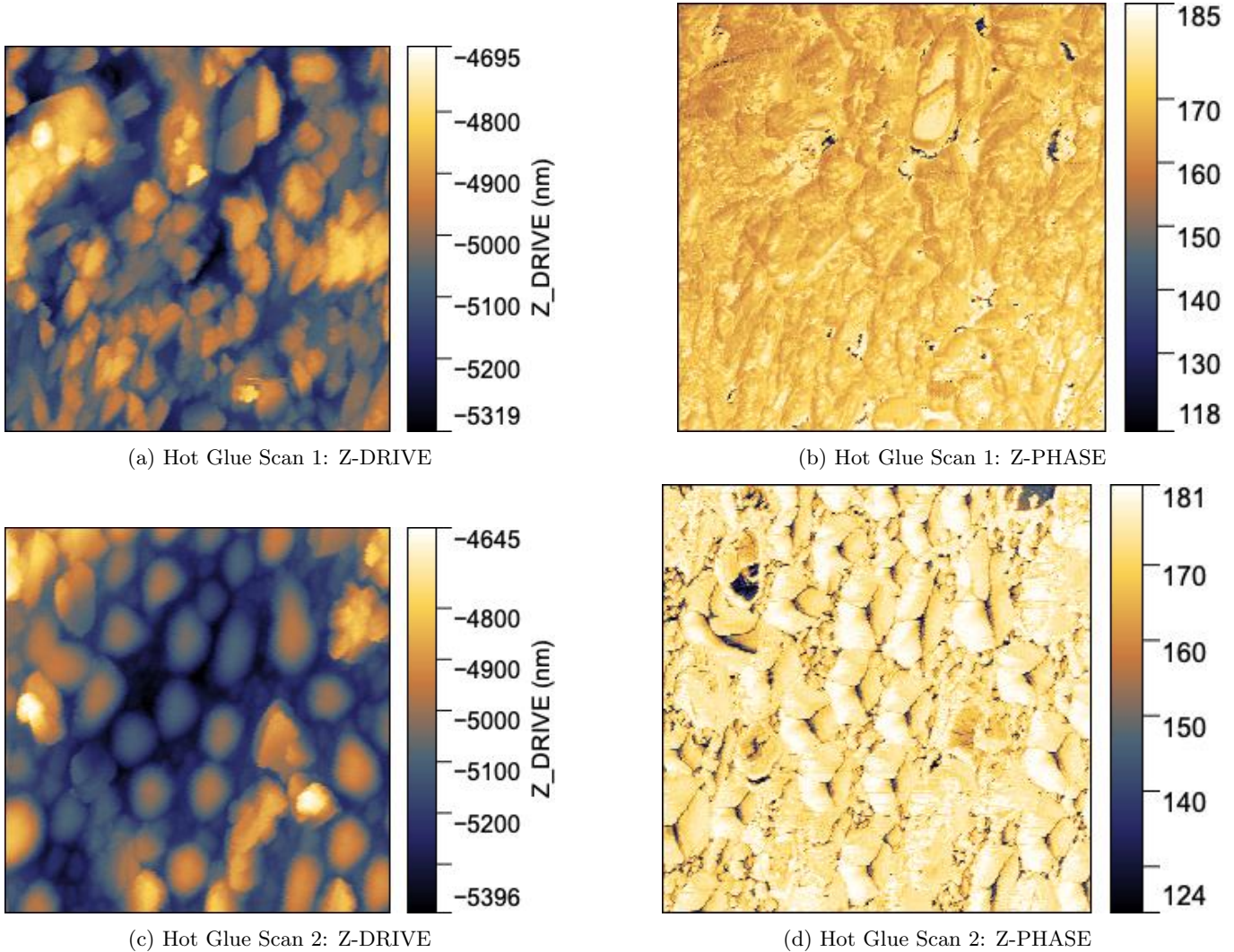


Figure 8: The hot glue has a largely irregular surface, as seen in the Z-DRIVE images. From some of the corresponding Z-PHASE imaging, we can make out different kinds of materials on the surface, especially in Scan 2. The existence of some polymers with a higher phase and lower phase can be seen in yellow, black and orange. We can make out at least 4 different polymers.

274 5. ANALYSIS

275 5.1. CD/DVD Experiment

276 For the CD, we found a track spacing of $1.71 \pm 0.06 \mu\text{m}$ between centers - nearly in agreement with the expected
 277 spacing of $1.6 \mu\text{m}$. We also find a track width of $1.04 \pm 0.06 \mu\text{m}$ and $0.67 \pm 0.03 \mu\text{m}$ between two tracks. The pit
 278 depth is approximately $135 \pm 20 \text{ nm}$. The high variation in the depth estimate is due to the slanting nature of the
 279 AFM sample as seen in Figure 7. These results are in agreement with the typical expectations for a CD, highlighted
 280 in Section 2.

281 Similarly, for the DVD we find a track spacing of $0.81 \pm 0.14 \mu\text{m}$ between centers - in agreement with the expected
 282 spacing of $0.74 \mu\text{m}$, the track width of $0.62 \pm 0.13 \mu\text{m}$ and $0.20 \pm 0.03 \mu\text{m}$ between two tracks. The pit depth is
 283 approximately $56 \pm 15 \text{ nm}$. This roughly agrees with expectations for DVDs as outlined in Section 2.

284 We used plane subtraction to obtain the accurate subtraction as line-by-line leveling would have created artificial
 285 results if the lines were in the same direction as the track spacing. The differences in height between the pits and

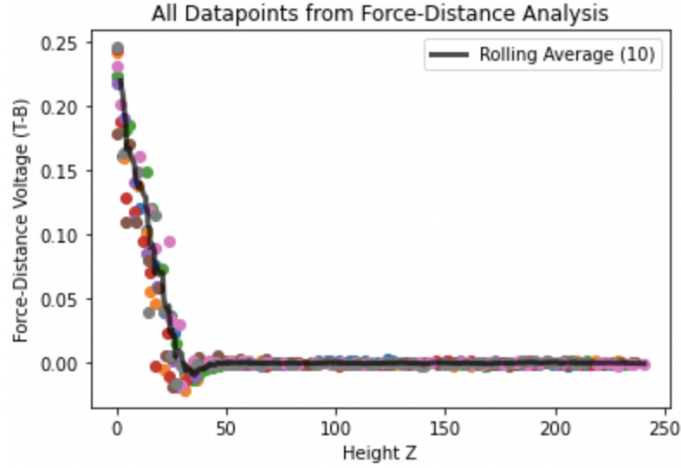


Figure 9: The force-distance graphs including the retraction and extension phase are aggregated in this diagram. We overplot a 10-window rolling average to more clearly identify the repulsive regime on the left, and the attractive regime on the right. Compare to Figure 2.

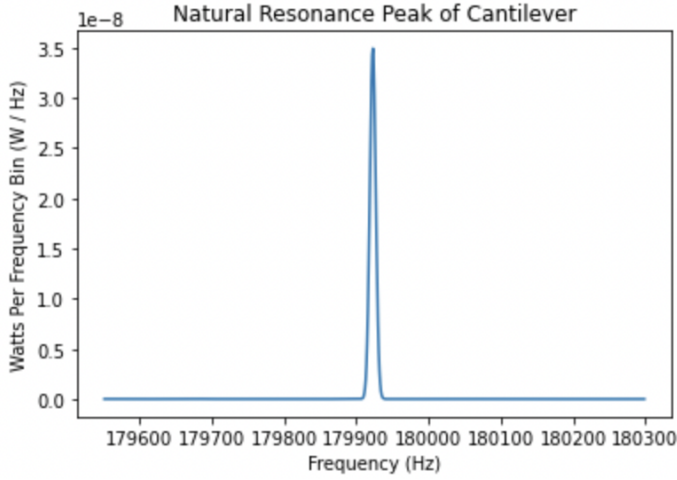


Figure 10: The Power Spectrum around the resonance peak. The integral of this power spectrum normalized by the gain gives us the cantilever deflection.

peaks would get cancelled out in their detection.

We estimate the information density of a CD as follows: since the length of a CD bit is $0.8 \mu m$, and the width is $1.6 \mu m$, the density is $0.78 \text{ bit}/\mu m^2$. Similarly, that of a DVD is $3.37 \text{ bit}/\mu m^2$, with a length of $0.4 \mu m$ and a width of $0.74 \mu m$.

5.2. Spring Constant Estimation

We estimate the spring constant of the cantilever using Lagrange interpolation over the points (0 kHz, 0 N/m), (160 kHz, 36 N/m), and (225 kHz, 90 N/m), as specified on the cover of the probe tip box. We find the interpolated value for 180kHz (our resonance frequency) and take the corresponding spring constant to be the correct value. The interpolation is shown in Figure 11.

With this procedure, we get an estimate of the spring constant as 49.96. This is a precise value, as the uncertainty in the Lagrange interpolation is unclear. That said, we can infer a rough upper and lower bound from the upper and lower bound of spring constant on the box: 36-90 N/m.

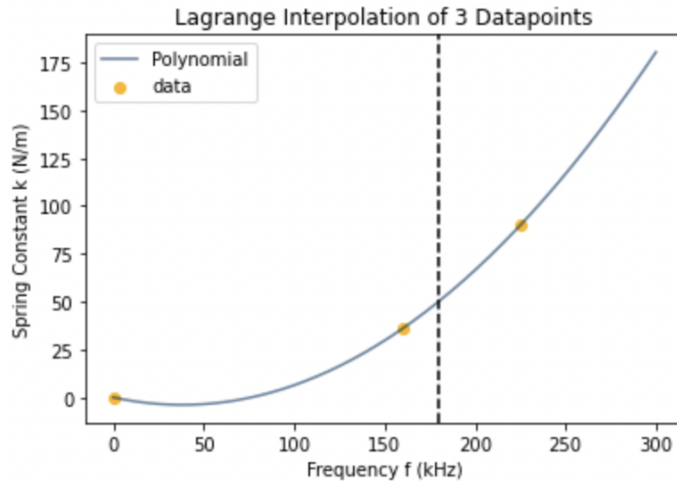


Figure 11: Lagrangian interpolation about the points $(0 \text{ kHz}, 0 \text{ N/m})$, $(160 \text{ kHz}, 36 \text{ N/m})$, and $(225 \text{ kHz}, 90 \text{ N/m})$, according to the probe box. The Lagrangian approximates the roughly square relationship between frequency and spring constant.

302 5.3. Boltzmann Constant Estimation

303 Using the mathematical techniques from Section 2 and the experimental setup and analysis from Section 3, 4, we
 304 get the power spectrum and the corresponding Gain, temperature, and spring constant. Applying the procedure, we
 305 find the integrated total power from the natural oscillation of the cantilever to be 369.4 nW.

306 The relationship between voltage V and the deflection z is linear, and the slope of this graph can be calculated from
 307 the repulsive regime of the force-distance graph 9. Selecting $Z < 35 \text{ nm}$ datapoints and fitting a line through them,
 308 we find the best fit slope to be $-6.10 \times 10^5 \text{ V/m}$ and the uncertainty estimated from the covariance matrix to be
 309 $0.36 \times 10^5 \text{ V/m}$.

311 Following 2, we find a RMS deflection $\langle z^2 \rangle$ of 9.96 pm or 0.0996 \AA . This is bounded by a lower uncertainty bound
 312 of 9.40 pm and an upper bound of 10.58 pm . In our reference Butt and Jashke 1995, we find that this measurement
 313 is in agreement with that expected for a spring constant of 50 N/m .

314 With a spring constant of 49.96 N/m , an RMS deflection of 9.96 pm , and a temperature $T = 295 \text{ K}$, we find
 315 the Boltzmann constant to be $k_B = 1.497_{-0.182}^{+0.218} \times 10^{23} \text{ J/K}$. This is in agreement with the Boltzmann constant of
 316 $1.38 \times 10^{23} \text{ J/K}$.

319 6. CONCLUSION AND FURTHER WORK

320 We accomplished 5 main goals in this experiment.

321 We analyzed the different sources of noise for the atomic force microscope and discovered that a decrease in the
 322 Z HV Gain and reduction in external noise significantly reduce the roughness and noise of the sample measurement.
 323 With both low noise and Z HV Gain of 5 rather than 15, we dropped the noise by a factor of 2.

324 We investigated a CD and DVD and confirmed that the track width, depth and spacing was in agreement with the
 325 standards for these CDs and DVDs. Indeed, we find that this was true. Most interestingly, we found that the track
 326 spacing of a CD is $1.71 \pm 0.06 \mu\text{m}$ between centers, while that of a DVD is $0.81 \pm 0.14 \mu\text{m}$. We also found that the
 327 information density of a DVD is 4.32 times larger.

328 The polymer glue was investigated for various polymers in its surface. We found over 4 different types of polymers,
 329 and that their distribution was largely independent of the height of the surface.

333 The Force-Distance graphs qualitatively agreed with the expected attractive and repulsive regime, and the repulsive
334 regime was successfully used to determine the slope mapping the T-B Voltage V and the cantilever deflections z . They
335 also allowed the successful calculation of the spring constant and the Boltzmann constant.

336
337 We estimated the Boltzmann constant using deflections of the cantilever, and found that the Boltzmann constant
338 was $k_B = 1.497^{+0.218}_{-0.182} \times 10^{23} J/K$, in agreement with the expected value within 1-sigma.

339
340 Future work from this experiment can be expanding the uses of the AFM beyond the variety of uses attempted in
341 this lab. For example, the AFM may be used in biophysics, underwater, and even to study interfacial water. The
342 errors in this experiment can be reduced by following a more careful approach, with a variety of different scans in
343 different areas of the samples, or by doing other different types of CDs and DVDs. Calibration could be improved by
344 performing an iterative calibration process until the data shows clear agreement with the calibration material. The
345 future of Atomic Force Microscopy hold much potential for our understanding of the nanometer to micrometer world.

REFERENCES

- 346 Min, G. 2022, in APS Meeting Abstracts, Vol. 2022, APS
347 March Meeting Abstracts, A73.001